Available online at www.sciencedirect.com
SCIENCE DIRECT
Polymer 46 (2005) 11407–11415
polymer
www.elsevier.com/locate/polymer

Suppression of inhomogeneities in hydrogels formed by free-radical crosslinking copolymerization

Nermin Orakdogen, Mine Yener Kizilay, Oguz Okay *

Department of Chemistry, Istanbul Technical University, 34469 Maslak, Istanbul, Turkey

Received 3 August 2005; received in revised form 21 September 2005; accepted 30 September 2005
Available online 24 October 2005

Abstract

Network microstructures of poly(acrylamide) (PAAm) and poly(*N*,*N*-dimethylacrylamide) (PDMA) hydrogels were compared by static light scattering and elasticity measurements. The hydrogels were prepared by free-radical crosslinking copolymerization of the monomers acrylamide (AAm) or *N*,*N*-dimethylacrylamide (DMA) with *N*,*N*′-methylenebis(acrylamide) as a crosslinker. During the formation of PAAm gels, the reaction time dependence of the scattered light intensity exhibits a maximum at a critical reaction time, while in case of PDMA gels, both a maximum and a minimum were observed, corresponding to the chain overlap threshold and the gel point, respectively. This difference in the time-course between the two gelling systems is due to the late onset of gelation in the DMA system with respect to the critical overlap concentration. Compared to the AAm system, no significant scattered light intensity rise was observed during the crosslinking polymerization of DMA. It was shown that, regardless of the crosslinker ratio and of the initial monomer concentration, PDMA gel is much more homogeneous than the corresponding PAAm gel due to the shift of the gelation threshold to the semidilute regime of the reaction system. The results suggest that the spatial gel inhomogeneity can be controlled by varying the gel point with respect to the critical overlap concentration during the preparation of gels by free-radical mechanism.

Keywords: Hydrogels; Gelation; Inhomogeneity

1. Introduction

Polymer networks around the gel point have been of interest for several years [1–4]. A polymer at its gel point is the critical gel and, is in a transition state between liquid and solid. The polymer approaches the gel point at a critical extent of reaction, i.e. at a critical monomer conversion x_{cr}. The polymer before the gel point, $x < x_{cr}$, is called a sol and beyond the gel point, $x_{cr} < x$, is called a gel. Free-radical crosslinking copolymerization (FCC) has been widely used to synthesize polymer gels. Since the lifetime of a growing radical during FCC is usually less than 1 s compared to the relatively long reaction times, radicals are continuously generated or terminated. The polymer chains formed during FCC are initially in a highly dilute solution so that the polymer concentration c is below the so-called overlap threshold c^* where the chains start to overlap. As the reactions proceed, c increases and, at $c = c^*$, the chains begin to be densely packed. When c becomes larger than c^*, a semidilute polymer solution forms in the reaction system, where the chains overlap and the average mesh size is the characteristic size of the entangled chains. Sol–gel transition during FCC may occur around the overlap concentration c^*, or later in the semidilute regime, depending on the synthesis parameters.

Sol–gel transition during FCC has mainly been investigated using the steady-state fluorescence and light scattering techniques. In the first technique, the transition is monitored by observing the intensity of an excited fluorescence probe during in situ fluorescence experiments [5]. However, it was shown later that this technique is insensitive to the sol–gel transition and, can only be used to monitor the onset of the gel effect in crosslinking polymerizations [6]. On the other hand, time-resolved light scattering technique provides valuable information about the gelation process [7–10]. In these experiments, the scattered light intensity at a fixed scattering angle is measured as a function of the reaction time; the gelation time is detected as the appearance of a speckle pattern due to the static concentration fluctuations in the gel [9,10]. Moreover, scattered light intensity profile during gelation is characterized by the appearance of a maximum, which was

* Corresponding author. Tel.: +90 212 2853156; fax: +90 212 2856386.
E-mail address: okayo@itu.edu.tr (O. Okay).

0032-3861/$ - see front matter © 2005 Elsevier Ltd. All rights reserved.
doi:10.1016/j.polymer.2005.09.082

ascribed to the reaction time at which the polymer concentration c in the reaction system attains the chain overlap concentration c^* [7].

It is well known that gelation and gel growth during FCC occur non-randomly due to the conversion and structure dependent reactivities of the functional groups as well as due to the cyclization and multiple crosslinking reactions [11,12]. Polymer gels formed in such a non-ideal picture necessarily include defects affecting their physical properties such as swelling, elasticity, transparency, and permeability. One of the network defects, which have been extensively studied, is the gel inhomogeneity [13,14]. In contrast to the ideal gels with a homogeneous distribution of crosslinks throughout the gel sample, real gels always exhibit an inhomogeneous crosslink density distribution, known as the spatial gel inhomogeneity. Since the gel inhomogeneity is closely connected to the spatial concentration fluctuations, scattering methods have been employed to investigate the spatial inhomogeneities [15–20]. The gel inhomogeneity can be manifested by comparing the scattering intensities from the gel and from a semidilute solution of the same polymer at the same concentration. The scattering intensity from gels is always larger than that from the polymer solution. The excess scattering over the scattering from polymer solution is related to the degree of the inhomogeneities in gels.

Spatial gel inhomogeneity in the final materials is undesirable for applications because structural inhomogeneity results in a dramatic reduction in the strength of the crosslinked materials. Although the inhomogeneity control in gels is quite sophisticated, the ionization of polymer gels is one of the methods used to suppress the inhomogeneities [13,14,21–25]. As the charge density of the network chains increases, they rearrange themselves as far as possible due to the repulsion of the charged groups as well as due to the inhomogeneous distribution of mobile counterions in the gel. Those of the chains in the dense regions of gel move apart to assume a new, less inhomogeneous structure. On the other hand, decreasing the crosslinker concentration used in the gel preparation also reduces the degree of spatial inhomogeneity due to the increasing distance between the pendant vinyl groups during the gelation process [26–29]. It should be noted that, Shibayama et al. recently observed an opposite behavior in the crosslink density dependence of spatial inhomogeneity in gels under a poor solvent condition [30]. In this case, the gel becomes more homogeneous as the degree of crosslinking is increased.

The effect of chemistry of the network chains on spatial gel inhomogeneity has not been reported before. The present study focuses on the problem of how to reduce the extent of spatial inhomogeneities in non-ionic gels by chemical means. Here, we investigated the formation processes of poly(acrylamide) (PAAm) and poly(*N*,*N*-dimethylacrylamide) (PDMA) gels by time-resolved light scattering. To convert the independent variable reaction time to the monomer conversion, dilatometric technique was also used to monitor the polymerization reactions. As will be seen below, we detected both a maximum and a minimum in the light scattering intensity profile during the formation of PDMA gels, corresponding to the overlap threshold and the gel point, respectively. Further, we demonstrate that PDMA gel is much more homogeneous than the conventional PAAm gel of the same effective crosslink density, due to the shift of the gelation threshold to the semidilute regime of the reaction system. Finally, we show that the spatial inhomogeneity can be controlled by varying the gel point with respect to the critical overlap concentration during the preparation of gels by free-radical mechanism.

2. Experimental section

2.1. Materials

Acrylamide (AAm, Merck), *N*,*N*-dimethylacrylamide (DMA, Fluka), *N*,*N*′-methylenebis(acrylamide) (BAAm, Merck), isopropyl alcohol (IPA, Merck), ammonium persulfate (APS, Merck), and *N*,*N*,*N*′,*N*′-tetramethylethylenediamine (TEMED) were used as received. APS and TEMED stock solutions were prepared by dissolving 0.080 g APS and 0.375 ml TEMED separately in 10 ml of water.

2.2. Crosslinking polymerization procedure

Free-radical crosslinking copolymerization reactions of AAm/BAAm and DMA/BAAm comonomer pairs were carried out in aqueous solutions at 21 °C in the presence of 3.51 mM APS initiator and 24.9 mM TEMED accelerator. Several sets of experiments were carried out. The gel synthesis parameters varied were the crosslinker ratio denoted by X (the mole ratio of BAAm to AAm or DMA) and the initial concentration of the monomers, C_0. The copolymerizations of DMA and BAAm were also conducted in the presence of various amounts of IPA as a chain transfer agent. The reactions were carried out in glass tubes, in the light scattering vials, as well as in glass dilatometers.

To illustrate the synthetic procedure in glass tubes, we give details for the preparation of a PDMA gel at $X = 1/82$ and $C_0 = 5$ w/v%: APS stock solution (1.00 ml), DMA (0.50 ml), BAAm (9.07 mg) and water (7.50 ml) were mixed in a 10 ml graduated flask. After bubbling nitrogen for 15 min, TEMED stock solution (1.0 ml) was added to the mixture. The solution was then poured into several glass tubes of 4.5–5 mm internal diameters and about 100 mm long. The glass tubes were sealed, and the polymerization was conducted at 21 °C for a predetermined reaction time. The gel samples thus obtained were subjected to the mechanical tests, as will be described below.

To monitor the scattered light intensity as a function of time, the crosslinking polymerizations were also carried out in the light scattering vials. All glassware was kept dustfree by rinsing in hot acetone prior using. The preparation of the reaction solutions and the polymerization procedure were similar as described above. The reaction solutions were filtered through membrane filters (pore size = 0.2 μm) directly into the vials. This process was carried out in a dustfree glovebox. All the solutions subjected to light scattering measurements were clear

and appeared homogeneous to the eye. The time evaluation of the scattered light intensity was measured at 21 °C using a commercial multi-angle light scattering DAWN EOS (Wyatt Technologies Corporation) equipped with a vertically polarized 30 mW Gallium–arsenide laser operating at $\lambda = 690$ nm and 18 simultaneously detected scattering angles. The light scattering system was calibrated against a toluene standard (Rayleigh ratio at 690 nm $= 9.7801 \times 10^{-6}$ cm^{-1}, DAWN EOS software) . The scattered light intensities were recorded from a scattering angle $\theta = 90°$ as a function of the reaction time. It should be noted that, in these time dependent measurements, spatial averaging of the scattered light intensity from the reaction solutions cannot be done by rotating the vials between successive measurements. However, repeated measurements on a given reaction system showed that this effect is small and the deviations in the scattering data between two runs are smaller than the size of the symbols shown in Figs. 3,4, and 6.

For gel samples after one day of preparation, the scattered light intensities were recorded from angles $\theta = 14.5$–$163.3°$ which correspond to the scattering vector q range 3.1×10^{-4}–2.4×10^{-3} Å^{-1}, where $q = (4\pi n/\lambda)\sin(\theta/2)$, n is the refractive index of the medium. To obtain the ensemble averaged light scattering intensity of gels, eight cycles of measurements with a small rotation of the vial between each cycle were averaged. For the calculation of excess scattering from gels, all the crosslinking polymerizations were repeated under the same experimental conditions except that the crosslinker BAAm was not used [29].

Linear polymerizations of AAm and DMA were also carried out in dilatometers consisted of a blown glass bulb, approximately 25 ml in volume connected to a 30 cm length of 1.5 mm precision-bore capillary tubing with a ground-glass joint [31]. The radius of the capillary was calibrated using mercury. During the reactions, the meniscus of the liquid column in the capillary was read with a millimetric paper to 0.2 mm. The reproducibility of the kinetic data was checked by repeating the experiments as well as by the gravimetric measurement of the monomer conversions at certain time intervals [32–34]. The deviation in the time versus conversion data was always less than 3%. The conversion of monomers x at the reaction time t was calculated as

$$x = \frac{\pi r^2}{V_0 \alpha_C} \Delta h \tag{1}$$

where r is the radius of the capillary, V_0 is the volume of monomers in the dilatometer, α_C is the contraction factor, and Δh is the height change of the liquid column in the capillary between time zero and time t, respectively. The contraction factors α_C for AAm and DMA polymerizations were found by gravimetric determination of the monomer conversions as 0.330 and 0.245, respectively.

2.3. Characterization of linear polymers

Linear PAAm and PDMA were isolated after a reaction time of 18 h by precipitation of the diluted reaction solutions in acetone. They were then dried in vacuum at room temperature to constant weight. Solutions of the polymers with concentrations in the range of 5×10^{-5} to 3×10^{-4} g/ml in water and in 0.1 M NaCl were prepared from the dry polymer samples. The solutions were filtered as described above and light scattering measurements were carried out using the DAWN EOS at $\lambda = 690$ nm and at scattering angles between 51 and 121°. The refractive index increment dn/dc was determined using the same polymer solutions using DAWN Optilap DSP at 690 nm. dn/dc values of the polymers in water were found as 0.163 and 0.166 ml/g for PAAm and PDMA, respectively. dn/dc of the polymers in 0.1 M NaCl cannot be measured due to the large voltages resulting from the NaCl present in salt solutions, which masked any voltage contributions made by the polymer. The weight-average molecular weight $\bar{M}_w$ and the radius of gyration $\langle R_g^2 \rangle^{1/2}$ of the polymers obtained from the Zimm plots are collected in the second and third columns of Table 1, respectively.

2.4. Gel points

Gel point measurements were carried out in light scattering vials containing the reaction solution and a PTFE-covered steel sphere [33,34]. The record of the reaction time was started after crossing the induction period, at which an abrupt increase in the scattered light intensity was observed (Figs. 2–4). The midpoint between the last time at which the sphere moved magnetically and that at which it stopped moving was taken as the gel point.

2.5. Mechanical measurements

All the mechanical measurements were conducted in a thermostated room of 21 ± 0.5 °C. Uniaxial compression measurements were performed on gel samples prepared in

Table 1
Characteristics of the linear PAAm and PDMA

Polymer	$10^{-6}\,\bar{M}_w$ (g/mol)		$\langle R_g^2 \rangle^{1/2}$ (nm)		c^* (g/100 ml)	
	In water	In 0.1 M NaCl	In water	In 0.1 M NaCl	In water	In 0.1 M NaCl
PAAm	0.91 (0.04)	0.97[a] (0.05)	66 (2)	55[a] (3)	0.13	0.23
PDMA	–[b]	2.4[a] (0.2)	–[b]	95[a] (3)	–[b]	0.11

$\bar{M}_w$ and $\langle R_g^2 \rangle^{1/2}$ are the weight average molecular weight and radius of gyration of the polymers, respectively, c^* is the overlap concentration calculated using Eq. (2). The numbers in parenthesis are the standard deviations.

[a] Calculated using dn/dc of the polymers in water.

[b] Not measured.

glass tubes at predetermined reaction times. For this purpose, the gels in the form of rods of about 4 mm in diameter were cut into samples of about 10 mm length. Then, each cylindrical gel sample was placed on a digital balance [35,36]. A load was transmitted vertically to the gel through a road fitted with a PTFE end-plate. The force acting on the gel was calculated from the reading of the balance m as $F=mg$, where g is the gravitational acceleration. The resulting deformation $\Delta l = l_0 - l$, where l_0 and l are the initial undeformed and deformed lengths, respectively, was measured using a digital comparator (IDC type Digimatic Indicator 543–262, Mitutoyo Co.), which was sensitive to displacements of 10^{-3} mm. The force and the resulting deformation were recorded after 20 s of relaxation. The measurements were conducted up to about 20% compression. The deformation ratio α (deformed length/initial length) was calculated as $\alpha = 1 - \Delta l/l_0$. The corresponding stress f was calculated as $f = F/A$, where A is the cross-sectional area of the specimen, $A = \pi r_0^2$, where r_0 is its initial radius. The elastic modulus G_0 of gels just after their preparation was determined from the slope of linear dependence $f = G_0(\alpha - \alpha^{-2})$. It should be noted that, to obtain the modulus of gels as a function of the reaction time, only six records were taken during the elasticity tests, which required 2 min. The reaction time was taken as the time period between the onset of the polymerization reactions (end of the induction period) and the start of the compression of the gel sample.

3. Results and discussion

3.1. Linear polymerization

We first monitored the polymerization reactions in the absence of the crosslinker BAAm by both dilatometry and light scattering. The initial monomer concentration C_0 was kept as 5 w/v%. The results of the dilatometric measurements are shown in Fig. 1 where the fractional monomer conversion x is plotted against the reaction time t in AAm (filled symbols) and DMA (open symbols) polymerizations. The duration of the induction period was found to be 5 and 15 min in AAm and DMA polymerizations, respectively. By repeated measurements, a variation of ± 2 min was observed in the induction period. The polymerization rate was however unchanged from these variations. The prolonged induction period in DMA polymerization is due to the presence of the inhibitor hydroquinone monomethylether in the DMA monomer. Addition of the same inhibitor into the AAm polymerization system also prolonged the induction period without changing the time-conversion curve. In the following, the reaction time is defined as the total time elapsed minus the time needed for the induction period. Fig. 1 also shows that the complete monomer conversions were obtained after a reaction time of 90 min and, the polymerization rates are almost equal for AAm and DMA polymerizations.

Fig. 2(A) shows the scattered light intensity I_s recorded at $\theta = 90°$ as a function of reaction time in linear AAm and DMA polymerizations. For comparison, conversion curves are also shown in Fig. 2(B). As expected, no intensity rise was observed

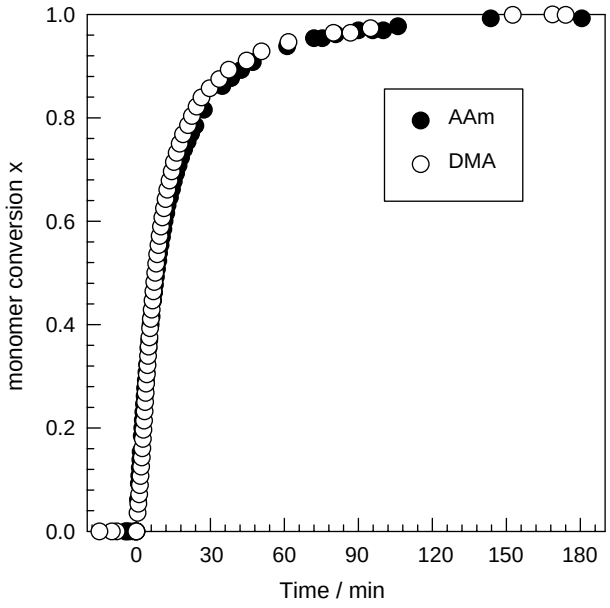

Fig. 1. The fractional monomer conversion x plotted against the reaction time in linear AAm (filled symbols) and DMA (open symbols) polymerizations. $C_0 = 5\%$.

during the induction period of the reactions. The start of the polymerization is accompanied with a rapid increase in I_s, which reaches a maximum after 0.6 and 0.4 min for AAm and DMA polymerizations, respectively. After passing the maximum intensity, I_s gradually decreases with the reaction time or monomer conversion and finally, attains a plateau value after about 10 min or 60% monomer conversion. As seen from Fig. 2(B), the maximum intensity occurs at a monomer conversion $x = 0.04 \pm 0.02$, indicating that the polymer concentration in the reaction system is 0.2 ± 0.1 w/v%. The maximum in the scattering curves can be interpreted as the point at which the polymer concentration in the reaction system attains the critical overlap concentration c^* [7]. c^* (in w/v%) can be calculated as [2]:

$$c^* = \frac{\bar{M}_w/N_A}{\left(\frac{4}{3}\pi\langle R_g^2\rangle^{3/2}\right)} 10^2 \qquad (2)$$

where N_A is the Avogadro's number. Using $\bar{M}_w$ and $\langle R_g^2\rangle^{1/2}$ of the polymers listed in Table 1 together with Eq. (2), the overlap concentrations c^* were calculated and are shown in the last column of Table 1. For the PAAm solution in water, $c^* = 0.13$, indicating that the reaction system attains this concentration at $x = 0.026$. Thus, c^* for the PAAm system is close to the polymer concentration of AAm reaction system at the peak maximum. Further, c^* for PDMA in salt solution is about half of that found for PAAm system (Table 1). Therefore, the maximum intensity in the DMA system appears earlier, i.e. in shorter reaction times.

The scattering curves shown in Fig. 2(A) can now be interpreted as follows: the rapid increase of I_s in short reaction times (<35 s) is due to the very short life time of radicals in FCC so that the polymer chains immediately start to form. Since a single polymer coil of a size 66 nm scatters light

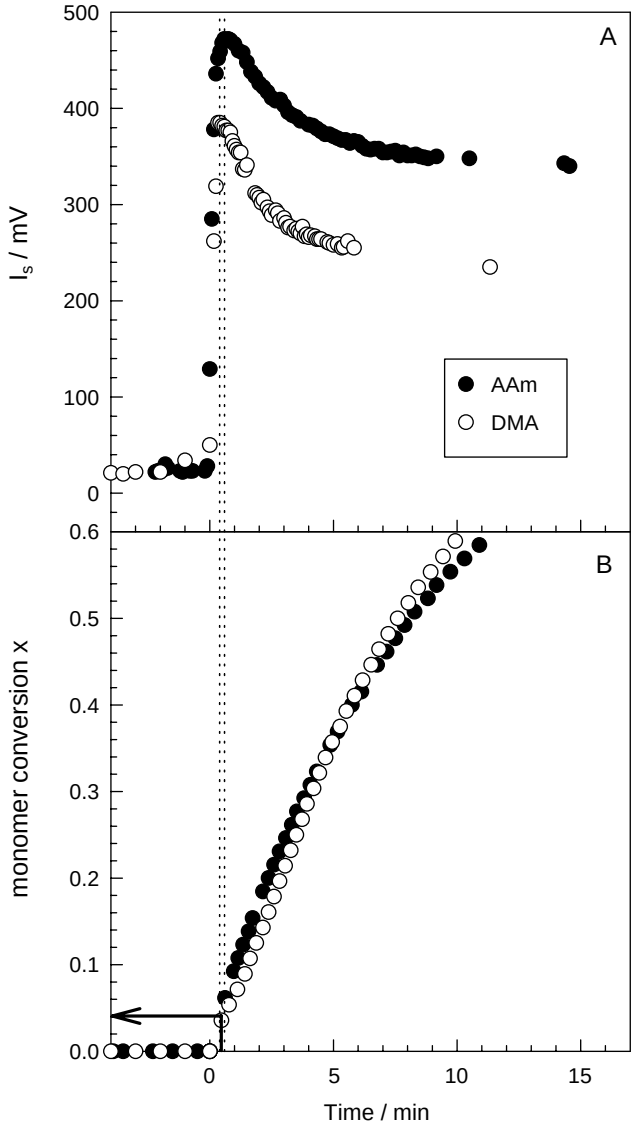

Fig. 2. The scattered light intensity I_s recorded at $\theta=90°$ (A) and the monomer conversion x (B) shown as a function of the reaction time in linear AAm (filled symbols) and DMA polymerizations (open symbols). $C_0=5\%$. The dotted vertical lines indicate the reaction times at the maximum intensity. The arrow shows the corresponding monomer conversion.

intensively, an abrupt intensity rise was observed with the onset of reactions due to the increasing number of coils with time. The number of individual polymer coils attains a maximum value at the overlap concentration c^* so that the scattering curve exhibits a peak at this concentration. In the semidilute regime, however, only the mesh size of the polymer solution is detectable by light scattering and not the size of the individual polymer coils. Since the mesh size is much smaller than the size of molecules, and it decreases further with increasing polymer concentration, I_s decreases with increasing reaction time, i.e. with the polymer concentration. Thus, the scattering curves display three regimes of the linear polymerization systems:

(1) Induction period ($x=0$).
(2) Dilute concentration regime ($x=0$ to about 0.04), and,
(3) Semidilute regime ($x>0.04$).

3.2. Crosslinking polymerization

Crosslinking polymerization reactions were carried out under the same reaction conditions as the corresponding linear polymerizations. Fig. 3 shows scattering intensity I_s versus reaction time plots, in a semi-logarithmic scale, for crosslinking AAm polymerization at two different initial monomer concentrations C_0 (A) and crosslinker ratios X (B). The shape of the curves is similar to those observed in linear polymerization. In accord with our previous work [29], the plateau value of the scattered light intensity I_s increases with decreasing monomer concentration due to the unfolding of concentration fluctuations in gels (A). I_s also increases with the crosslinker ratio X due to the increasing degree of spatial gel inhomogeneity on rising the crosslink density of gels in a good solvent (B). For reaction times longer than 10^3 min (>17 h), a decrease in the scattered light intensity was observed. This is due to the partial hydrolysis of AAm units of the network chains into acrylic acid units. As was shown before [23,37,38], the use of TEMED as the accelerator during the gelation process leads to the formation of charged groups in the aged

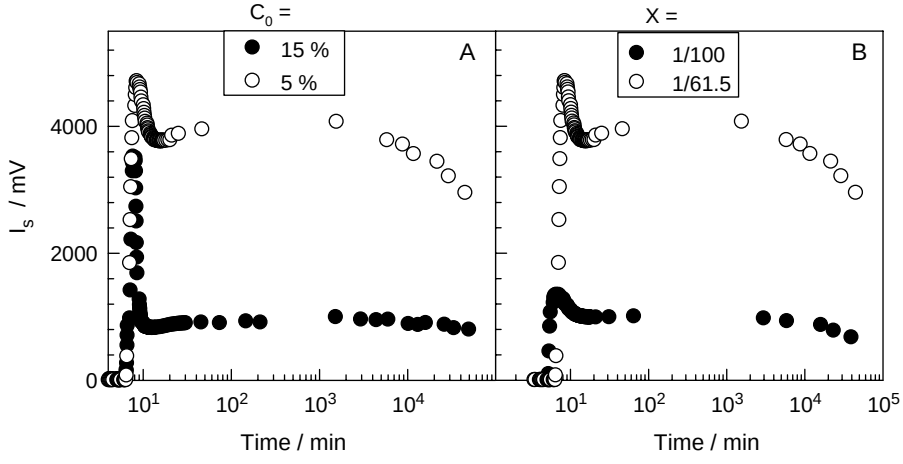

Fig. 3. The scattered light intensity I_s at $\theta=90°$ versus reaction time plots, in a semi-logarithmic scale, for crosslinking AAm polymerization. (A) $X=1/61.5$, $C_0=5$ (○) and 15% (●). (B) $C_0=5\%$, $X=1/61.5$ (○) and 1/100 (●).

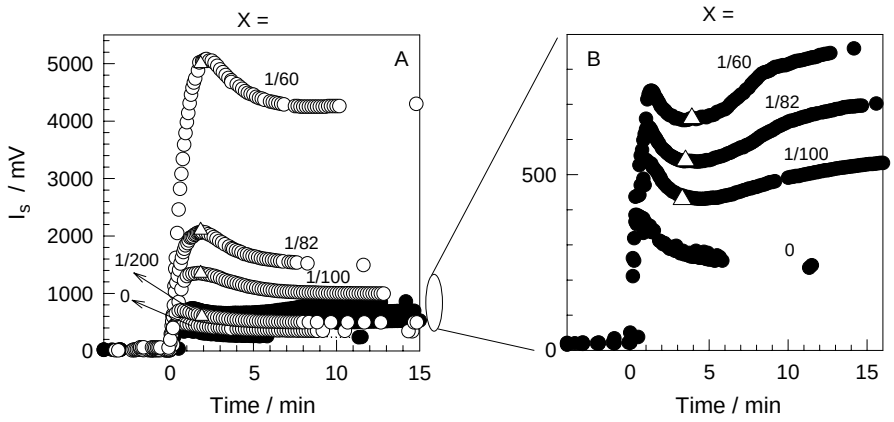

Fig. 4. The scattered light intensity I_s at $\theta = 90°$ plotted against the reaction time for crosslinking AAm (open symbols) and DMA polymerizations (filled symbols). $C_0 = 5\%$. The crosslinker ratios X are indicated in the figure. Figure B shows the magnified observation of the scattering curves of DMA polymerizations. The open triangles illustrate the gel points in terms of the reaction times.

PAAm gels, whose number increases with increasing aging time in the polymerization reactor. Since increasing charge density reduces the apparent degree of spatial gel inhomogeneity, I_s gradually decreases at longer reaction times. Thus, the scattering curves visualize the effects of various gel preparation parameters on the extent of spatial inhomogeneity in PAAm hydrogels.

In Fig. 4(A), the scattered light intensity I_s is plotted against the reaction time for crosslinking AAm (open symbols) and DMA polymerizations (filled symbols). Here, we varied the crosslinker ratio X between 1/200 and 1/60 keeping the total monomer concentration C_0 at 5 w/v%. The data obtained in linear polymerizations ($X = 0$) are also shown in the figure. The open triangles illustrate the gel points in terms of the reaction times. It should be noted that, in contrast to the classical gel point at which the system changes from liquid to solid-like state, the sol–gel transitions in both gelation systems occurred not abrupt and took about 30 s. Therefore, we define here the gel point as the average of two reaction times where the gel starts to form at the lower part of the reaction mixture and where the gel occupies the whole available volume. Several interesting features can be seen from the figure. For AAm polymerization, the shape of I_s versus time plots is the same with and without crosslinker. The larger is X the stronger is the increase of I_s, which is obviously due to crosslinking reactions prior to gelation leading to the formation of larger molecules. Moreover, the gel point in AAm crosslinking copolymerization is close to the reaction time at the peak position, indicating that gelation occurs at a polymer concentration in the vicinity of the chain overlap concentration c^*. A closer examination of Fig. 4(A) indicates however that gelation occurs below overlap at high crosslinker ratios while it occurs later at low values of the crosslinker ratios.

Surprisingly, no significant intensity rise was observed in the crosslinking polymerization of DMA (Fig. 4(A)). Moreover, Fig. 4(B), showing the magnified observation of the scattering curves of DMA polymerizations illustrates existence of both a maximum and a minimum in the scattering curves of the DMA system. A comparison of the gel points in AAm and DMA systems shows that the gel formation is retarded by replacing AAm with the DMA monomer. Further, gelation in the DMA system occurs at reaction times corresponding to the minima in the scattering curves. Similar to the AAm system, the larger the X, the stronger the scattered intensity I_s along the DMA polymerization. However, the intensity increase with the crosslinker ratio is much less than that observed in AAm polymerization.

One possible explanation for the reduced degree of scattered light intensity from PDMA gels is their lower effective crosslink density leading to a reduced degree of spatial inhomogeneity. In order to check this point, we conducted mechanical measurements on both PAAm and PDMA gels formed at various reaction times. The results are shown in Fig. 5 where the modulus of elasticity of gels G_0 prepared at

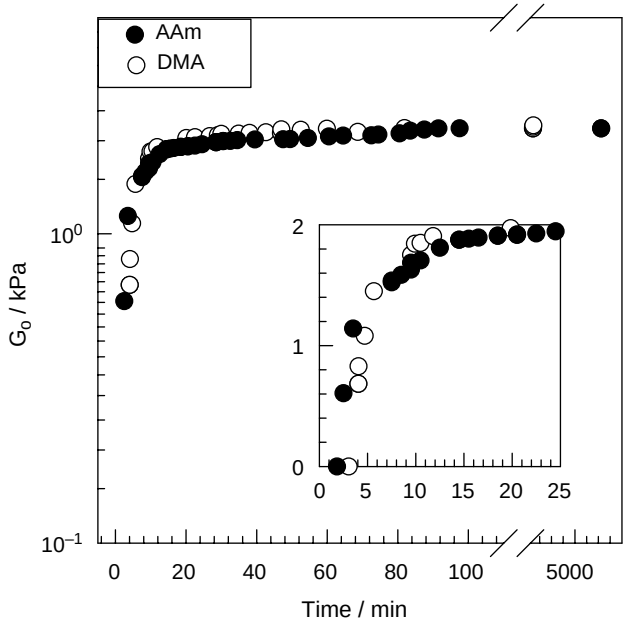

Fig. 5. The elastic modulus of gels after preparation G_0 plotted against the reaction time for crosslinking AAm (filled symbols) and DMA polymerizations (open symbols). $C_0 = 5\%$; $X = 1/82$. The inset shows the initial reaction period beyond gelation.

$X=1/82$ is plotted against the reaction time. It is seen that PDMA gels exhibit slightly larger elastic moduli compared to PAAm gels. The difference observed just beyond the gel point ($G_0<1$ kPa) shown in the inset is due to the early onset of gelation in AAm polymerization so that the growth of PAAm gel starts earlier. Similar results such as those in Fig. 5 were also obtained for gels prepared at different crosslinker ratios. For example, at $X=1/60$, the plateau value of G_0 was found to be 2.8 and 2.5 kPa for PDMA and PAAm gels, respectively. Thus, the reduced scattering from DMA system compared to the AAm system cannot be explained with the effect of the crosslink density. It is rather a result of very different microscopic structure of PDMA gel compared with that of PAAm gel. This difference is increasing with increasing crosslink density (Fig. 4(A)). A plausible explanation of this difference is the late onset of gelation in DMA polymerization. As seen in Fig. 4(B), although the molecular weight of the primary molecules is higher (Table 1), gelation occurs in the DMA system in the semidilute regime, while in the AAm system, it occurs around the overlap concentration. The delay of gelation in the DMA system is probably due to the bulky side groups of PDMA chains, which reduce the reaction rates between macromolecules. Thus, the crosslinking reactions between the growing PDMA chains and the pendant vinyl groups occur at a slower rate so that the gel point is shifted to higher conversions. The much higher molecular weight of polymers formed in the DMA polymerization compared to the AAm system (Table 1) is also a result of the reduced rate of terminations reactions. Indeed, previous work shows that the higher the DMA content of the comonomer feed in DMA/AAm copolymerization, the higher the molecular weight of the polymers [39].

Thus, for PAAm gels, microgel-like clusters form during the gelation process due to the extensive cyclization reactions as well as due to the different reactivities of AAm and BAAm monomers. As a result, PAAm represents a typical inhomogeneous gel formed by free-radical crosslinking mechanism. On the contrary, in DMA polymerization, a solution of linear and branched polymers crosses the semidilute regime prior to the onset of gelation and therefore, this system resembles gel formation from a preformed polymer solution. Since crosslinks are introduced relatively randomly in space during crosslinking of preformed polymer chains [13,40], PDMA gel is much more homogeneous than PAAm gel of the same effective crosslink density, so that it scatters much less light than the corresponding PAAm gel.

Moreover, the appearance of a minimum in the scattering curve of the DMA system is due to the increase of the gel elasticity during the post-gelation period of the reactions (Fig. 5). Since the spatial inhomogeneity becomes larger on raising the crosslink density, scattering intensity beyond the gel point increases up to a reaction time of 10 min due to the simultaneous increase of the elastic modulus (Fig. 5). The minima do not appear in the scattering curves of AAm system. This is due to the fact that the gelation time is close to the time at the peak maximum so that the increase in I_s due to the increasing modulus of gels is masked by the decrease in I_s due to the transition to the semidilute regime. Thus, the concentration effect decreasing the mesh size of polymer chains dominates over the crosslink density effect, resulting in a continuous decrease in I_s beyond the peak maximum in AAm polymerization.

According to these results, factors reducing the crosslink density of gels should also weaken the minima in the scattering curves of the DMA system. This behavior is indeed seen in Fig. 4(B), where the minima become weaker as the crosslinker ratio X is decreased. Moreover, addition of a chain transfer agent (CTA) in the DMA system should also reduce the intensity rise after the gel point so that the minima should disappear at high CTA concentrations. This is due to fact that CTA decreases the molecular weight of the primary molecules and therefore, gelation occurs later and the gels formed exhibit a lower modulus of elasticity with increasing amount of CTA [28,41]. In another set of experiments, we monitored crosslinking polymerization of DMA in the presence of various amounts of isopropyl alcohol (IPA) as a CTA, where the crosslinker ratio X was kept as 1/82 and the initial monomer concentration C_0 was chosen again as 5 w/v%. The scattering intensity I_s versus reaction time was monitored for all samples. The results are shown in Fig. 6. As expected, the gelation times are shifted to larger values as the IPA content is increased. For example, gelation times were 3.9, 7, and 12 min for 0, 2.50, and 3.01 mol IPA/mol DMA, respectively. As seen from the figure, the shift of the gel point is accompanied with a gradual disappearance of the minimum of the scattering curves. Simultaneously, the initial rise of I_s in the dilute regime becomes smaller due to the decreasing molecular weight of sol molecules.

The results thus obtained show that PDMA gels formed at $C_0=5\%$ and up to a reaction time of 15 min are less

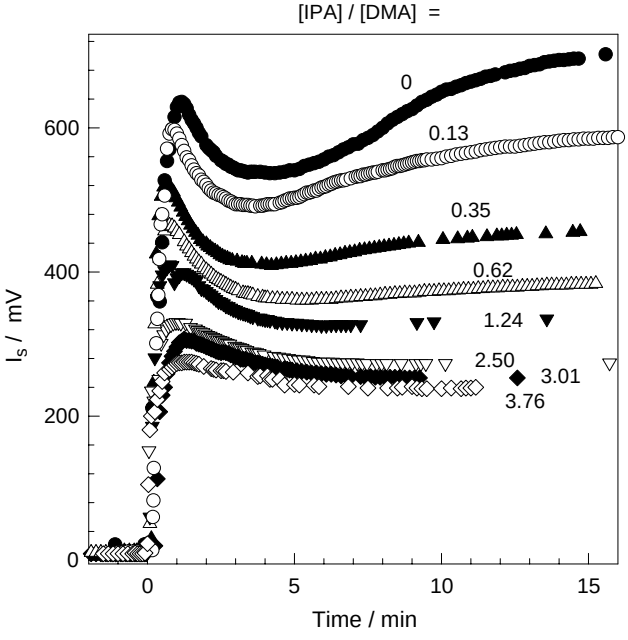

Fig. 6. The scattered light intensity I_s at $\theta=90°$ plotted against the reaction time for crosslinking DMA polymerizations in the presence of various amounts of IPA. $C_0=5\%$. $X=1/82$. The mole ratios of IPA to BAAm are indicated.

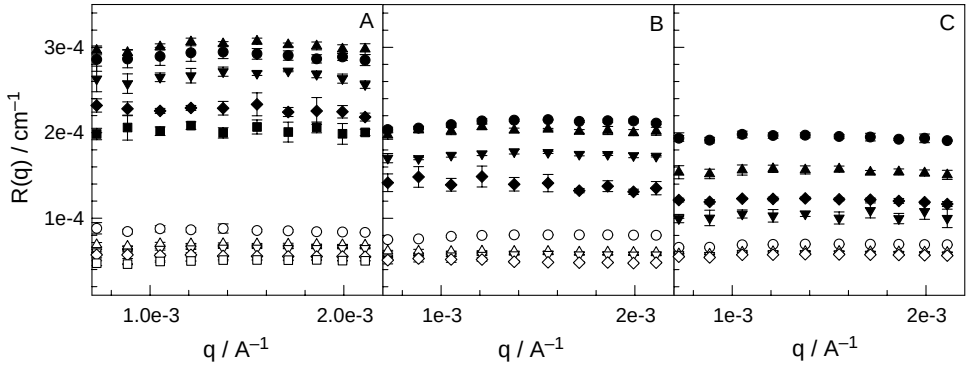

Fig. 7. Rayleigh ratio $R(q)$ versus scattering vector q plots for the PDMA gels (filled symbols) and for the corresponding linear PDMA solutions (open symbols). (A) $X=1/60$, $C_0=2.4$ (●, ◯), 3.6 (▲, △), 4.2 (▼, ▽), 6.1 (◆, ◇), 7.3% (■, □). (B) $X=1/82$, $C_0=2.4$ (●, ◯), 4.7 (▲, △), 5.3 (▼, ▽), 7.3% (◆, ◇). (C) $X=1/100$, $C_0=3.6$ (●, ◯), 4.7 (▲, △), 6.1 (▼, ▽), 7.3% (◆, ◇).

inhomogeneous compared to PAAm gels. In order to generalize this finding, we monitored the scattered light intensity from a series of PDMA gels formed at various initial monomer concentrations and crosslinker ratios. The reaction time was set to 24 h. Fig. 7 shows the Rayleigh ratio $R(q)$ versus the scattering vector q plots for PDMA gels at three different crosslinker ratios (filled symbols) and for the corresponding linear PDMA solutions (open symbols). The initial monomer concentrations C_0 are indicated in the figure caption. For both gels and solutions, the light scattering intensity does not change much with the scattering vector q. This is expected since we are in the semidilute regime for PDMA solutions and we are probing length scales large compared with those typical for polymer gels. Therefore, in the following paragraphs, we focus on the scattering intensities measured at a fixed scattering vector $q=1\times10^{-3}$ Å^{-1}. Fig. 7 also shows that the scattering intensity from gels is larger than that from the polymer solution. The excess scattering over the scattering from polymer solution $R_{ex,q}$ was calculated as:

$$R_{ex,q} = R_{gel,q} - R_{sol,q} \tag{3}$$

where $R_{gel,q}$ and $R_{sol,q}$ are the Rayleigh ratios for gel and polymer solution at a fixed scattering vector q, respectively. Fig. 8 shows the excess scattering $R_{ex,q}$ (filled symbols) of PDMA gels plotted as a function of C_0. For comparison, excess scattering data reported for PAAm gels [29,42] formed at various concentrations and crosslinker ratios are also shown in Fig. 8 by the open symbols. It is seen that the excess scattering from PDMA gels is about tenfold smaller that that from PAAm gels. Since the thermal concentration fluctuations in gels are eliminated in Eq. (3), excess scattering is a measure of the degree of spatial inhomogeneities. Thus, the results demonstrate the homogeneity of PDMA gels, regardless of the crosslinker ratio and of the monomer concentration, compared to the PAAm gels formed under identical conditions.

In order to elucidate the origin of the different microstructures of PDMA and PAAm gels, we employed the statistical theory proposed by Panyukov and Rabin for describing the structure factors for gels [43,44]. The theory assumes that the gel is prepared by instantaneous crosslinking of semidilute polymer solutions. Despite these limitations to the applicability of the Panyukov–Rabin theory, it is the only available theory predicting the degree of spatial inhomogeneities in gels from their preparation conditions, i.e. from their history [24,25,29,30,40,42,45–48]. Respective calculations using the experimental time-conversion (Fig. 2(B)) and time modulus data (Fig. 5) showed that the value of the dimensionless effective second virial coefficient w_0 at gel preparation plays an essential role in the degree of spatial inhomogeneity of the present gels. Assuming that the gel is in a good solvent (the scaling) regime, w_0 is given by [43,44]

$$w_0 = (\nu_2^0)^{5/4} N \tag{4}$$

where ν_2^0 is the volume fraction of crosslinked polymer in the gel just after preparation, and N is the number of segments between two successive crosslinks. According to Eq. (4), the degree of dilution of crosslinked polymer together with the effective crosslink density determines the second virial

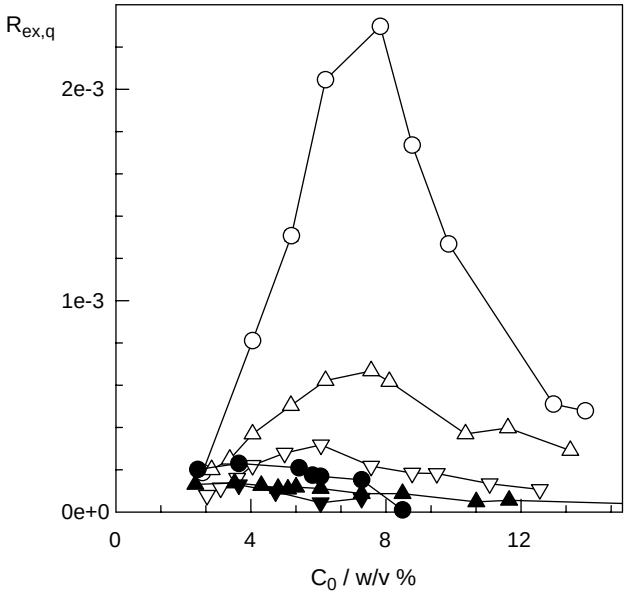

Fig. 8. The excess scattering $R_{ex,q}$ measured at $q=1\times10^{-3}$ Å^{-1} shown as a function of the initial monomer concentration C_0 for PDMA hydrogels (filled symbols). For comparison, excess scattering $R_{ex,q}$ data for PAAm gels taken from the literature [29,42] are also shown in the figure by the open symbols. $X=1/60$ (●,◯), 1/66 (▲, △), and 1/100 (▼,▽).

coefficient w_0. The increasing polymer concentration ν_2^0 at a constant crosslink density leads to a more positive value of w_0 and suppresses density fluctuations in the gel. In the present case, the late gelation in the crosslinking DMA polymerization produces a gel that is much more concentrated than that formed in the AAm polymerization so that DMA gels exhibit a lesser degree of inhomogeneity. The physical meaning of the effect of w_0 on the spatial gel inhomogeneity is that an effective positive second virial coefficient leads to repulsion between the network chains (similar to the repulsion between the charged chains), and therefore, masks the inhomogeneities. The results thus suggest that the spatial inhomogeneity in gels formed by FCC can be controlled by varying the gel point with respect to the critical overlap concentration during the gel preparation stage.

4. Conclusions

The formation processes of PAAm and PDMA gels were investigated by time-resolved light scattering. The hydrogels were prepared by free-radical crosslinking copolymerization of the monomers AAm or DMA with BAAm as a crosslinker. During the formation of PAAm gels, the reaction time dependence of the scattered light intensity exhibits a maximum at a critical reaction time or monomer conversion. However, the scattering intensity profile during the formation of PDMA gels exhibits both a maximum and a minimum, corresponding to the overlap threshold and the gel point, respectively. This difference in the time-course between the two gel formation systems is due to the late onset of gelation in the DMA system with respect to the critical overlap concentration. Compared to the AAm system, no significant scattered light intensity rise was observed during the crosslinking polymerization of DMA. The results show that PDMA gels are much more homogeneous than the corresponding PAAm gels due to the shift of the gelation threshold to the semidilute regime of the reaction system. Thus, the spatial gel inhomogeneity can be controlled by varying the gel point with respect to the critical overlap concentration during the preparation of gels by free-radical mechanism.

References

[1] Flory PJ. Principles of polymer chemistry. Ithaca, NY: Cornell University Press; 1953.
[2] De Gennes PG. Scaling concepts in polymer physics. Ithaca, NY: Cornell University Press; 1979.
[3] Dusek K. Makromol Chem Suppl 1979;2:35.
[4] Stauffer D, Coniglio A, Adam M. Adv Polym Sci 1982;44:103.
[5] Pekcan O, Yilmaz Y, Okay O. Chem Phys Lett 1994;229:537.
[6] Okay O, Kaya D, Pekcan O. Polymer 1999;40:6179.
[7] Norisuye T, Shibayama M, Nomura S. Polymer 1998;39:2769.
[8] Lesturgeon V, Nicolai T, Durand D. Eur Phys J 1999;B9:71.
[9] Boyko V, Richter S. Macromol Chem Phys 2004;205:724.
[10] Shibayama M, Ozeki S, Norisuye T. Polymer 2005;46:2381.
[11] Funke W, Okay O, Joos-Muller B. Adv Polym Sci 1998;136:139.
[12] Okay O. Prog Polym Sci 2000;25:711.
[13] Bastide J, Candau SJ. In: Cohen Addad JP, editor. Physical properties of polymeric gels. New York: Wiley; 1996. p. 143.
[14] Shibayama M. Macromol Chem Phys 1998;199:1.
[15] Mallam S, Horkay F, Hecht AM, Geissler E. Macromolecules 1989;22:3356.
[16] Ikkai F, Shibayama M. Phys Rev E 1997;56:R51.
[17] Cohen Y, Ramon O, Kopelman IJ, Mizraki S. J Polym Sci, Polym Phys Ed 1992;30:1055.
[18] Schosseler F, Skouri R, Munch JP, Candau SJ. J Phys II 1994;4:1221.
[19] Shibayama M, Tanaka T, Han CC. J Chem Phys 1992;97:6842.
[20] Horkay F, McKenna GB, Deschamps P, Geissler E. Macromolecules 2000;33:5215.
[21] Moussaid A, Candau SJ, Joosten JGH. Macromolecules 1994;27:2102.
[22] Skouri R, Schosseler F, Munch JP, Candau SJ. Macromolecules 1995;28:197.
[23] Kizilay MY, Okay O. Polymer 2003;44:5239.
[24] Yazici I, Okay O. Polymer 2005;46:2595.
[25] Ikkai F, Shibayama M. J Polym Sci, Part B: Polym Phys 2005;43:617.
[26] Hecht AM, Duplessix R, Geissler E. Macromolecules 1985;18:2167.
[27] Shibayama M, Ikkai F, Nomura S. Macromolecules 1994;27:6383.
[28] Cerid H, Okay O. Eur Polym J 2004;40:579.
[29] Kizilay MY, Okay O. Macromolecules 2003;36:6856.
[30] Shibayama M, Ikkai F, Shiwa Y, Rabin Y. J Chem Phys 1997;107:5227.
[31] Okay O, Naghash HJ, Capek I. Polymer 1995;36:2413.
[32] Okay O, Kurz M, Lutz K, Funke W. Macromolecules 1995;28:2728.
[33] Naghash HJ, Okay O. J Appl Polym Sci 1996;60:971.
[34] Durmaz S, Okay O. Polymer 2000;41:3693.
[35] Sayil C, Okay O. Polymer 2001;42:7639.
[36] Gundogan N, Melekaslan D, Okay O. Macromolecules 2002;35:5616.
[37] Tanaka T. Phys Rev Lett 1978;40:820.
[38] Ilavsky M, Hrouz J, Stejskal J, Bouchal K. Macromolecules 1984;17:2868.
[39] Hocking MB, Klimchuk KA, Lowen S. J Polym Sci, Part A: Polym Chem 2000;38:3128.
[40] Norisuye T, Masui N, Kida Y, Ikuta D, Kokufuta E, Ito S, et al. Polymer 2002;43:5289.
[41] Okay O, Balimtas NK, Naghash HJ. Polym Bull 1997;39:233.
[42] Kizilay MY, Okay O. Polymer 2004;45:2567.
[43] Panyukov S, Rabin Y. Macromolecules 1996;29:7960.
[44] Rabin Y, Panyukov S. Macromolecules 1997;30:301.
[45] Ikkai F, Iritani O, Shibayama M, Han CC. Macromolecules 1998;31:8526.
[46] Takata S, Norisuye T, Shibayama M. Macromolecules 2002;35:4779.
[47] Gundogan N, Okay O, Oppermann W. Macromol Chem Phys 2004;205:814.
[48] Nie J, Du B, Oppermann W. Macromolecules 2004;37:6558.